

Article

# Effects of Island-Coated PVdF-HFP Composite Separator on the Performance of Commercial Lithium-ion Batteries

**Junhua Zhao** <sup>1,\*</sup>, **Qin Hu** <sup>2</sup>, **Jun Wang** <sup>3</sup>, **Pinjie Zhang** <sup>4</sup>, **Youliang Zhu** <sup>1</sup>, **Guoqiang Wu** <sup>1</sup>, **Yanwen Lv** <sup>1</sup>, **Liang Lv** <sup>1</sup>, **Yongjin Zhao** <sup>1</sup> and **Meiting Yang** <sup>1</sup>

<sup>1</sup> College of Chemical and Material Engineering, Quzhou University, Quzhou 324000, Zhejiang, China; uglyzhu@163.com (Y.Z.); zjwgq@163.com (G.W.); qzlyw@qzu.zj.cn (Y.L.); lianglv\_buct@126.com (L.L.); 18868083979@163.com (Y.Z.); 15700011697@163.com (M.Y.)

<sup>2</sup> Zhejiang Green New Materials Co., Ltd., Quzhou 324000, Zhejiang, China; huqin08@163.com

<sup>3</sup> MEET Battery Research Center, Institute of Physical Chemistry, University of Muenster, Muenster 48149, Germany; jun.wang@uni-muenster.de

<sup>4</sup> Zhejiang Juhua Co., Ltd., Quzhou 324004, Zhejiang, China; zhangpinjeyx@163.com

\* Correspondence: qzzjh@qzu.zj.cn; Tel.: +86-570-802-6552

Received: 31 August 2018; Accepted: 26 November 2018; Published: 28 November 2018



**Abstract:** The widespread industrialization of high-energy density commercial lithium-ion batteries has long been challenged by issues of safety and efficiency stemming from uncontrollable lithium dendritic growths. Here, an island-coated composite separator has been fabricated using a pre-swelling process with water-based dispersions to address the issue of dendrite growth. The pre-swelling of the polymer particle surface balances the contradiction between the high crystallinity and electrolyte compatibility showing high electrolyte wettability and electrolyte uptake ability. Furthermore, the point-to-point surface structure can balance the high interfacial adhesion of electrodes and anti-deformation ability well, which is beneficial for preventing ripple-shaped and pot-shaped deformation, smoothing the solid particle morphology of the electrode and achieving a steady interfacial structure for lithium diffusion in cells. This new strategy constructs a non-continuous novel structure, achieving greatly improved dendrite growth suppressing and cell interface stabilization. This paper has opened up a new method for the development of low cost, simple process and easy industry of the lithium-ion pouch cell with improved quality and efficiency.

**Keywords:** lithium dendrite; island-coated separator; pre-swelling process; composite; lithium-ion batteries

## 1. Introduction

Secondary lithium-ion batteries (LIB) are currently widely used in electronics, electric vehicles, and energy storage systems, due to their superior properties, such as high energy density, long cycle life, and high operational voltage [1–6]. Increasing demand for LIB with high energy and power density drives the improvement of lithium battery design, such as development of high-energy storage systems and optimization of electrode structure or design parameters [2,3]. However, the formation of uncontrolled dendritic and mossy lithium on the anode surface leads to low capacity retention and serious safety concerns [4–7], such as thermal runaway or even fire/explosion of the battery [8]. Lithium dendrite is formed near the edge of the anode by asymmetrical lithium-ion conductivity and mechanical stress, which can be described by the classical deposition/dissolution model [7]. Based on this model, two categories of methods are given for suppressing the growth of lithium dendrite: interface modification and manufacturing three-dimensional (3D) pore structure. Many

efforts have been devoted successfully to suppressing lithium dendrite, including surface-treated anode, modification electrolyte, and novel separator/anode structure, etc. [4–7]. However, most of those strategies have a complex process of synthesis or electrochemical control, which is hard for industrial application.

Composite separators remain one of the few effective ways of industrial production, because of their versatility, simpleness, and high efficiency [9–14]. PVdF-based polymer-coated composite separator (PPCS) is convenient for ionic transformation ( $\text{Li}^+$ ) diffusion because of lower interfacial resistance and higher ionic conductivity [9,10]. Dendrite growth can be efficiently monitored by in-situ voltage observation between the metallic interlayer of the polyethylene (PE) separator and electrode [13]. However, a PPCS is synthesized mainly using a solution casting technique and phase inversion technique [15,16], using organic solvents and being sensitive to temperature and humidity level, which result in environmental pressure and compromised function. The higher the compatibility of separator to the electrolyte, the lower the crystallinity of the polymer [17]. This results in the decrease of mechanical moduli and electrochemical stability in the electrolyte. In addition, the strong surface bonding between anode and separator suffers from poor yield upon repeated charge-discharge cycles due to the battery deformation. Therefore, to solve the notorious dendrite growth problem, it is desirable to find a proper low-cost industrialization process with homogeneous and stable interface concurrently.

Herein, a polymer island-coated (PIC) separator is designed and synthesized using a pre-swelling process with water-based dispersions. The contradiction between high crystallinity and electrolyte compatibility is balanced by the pre-swelling of the polymer particle surface, and the unique island-like surface structure can balance the high interfacial adhesion of electrodes and anti-deformation ability well. The effect mechanism of a PIC separator on the suppression of dendrite growth and stabilization of interface is studied.

## 2. Materials and Methods

Polyethylene (PE) membrane (40% porosity, 9  $\mu\text{m}$  thickness, Toray, Tokyo, Japan) and polyacrylate (PA) binder were kindly provided by Cube Energy Technology Co., Ltd., Dongguan, Guangdong, China. Poly(vinylidenefluoride-co-hexafluoropropylene) (PVdF-HFP) was purchased from Kynar, Arkema, Colombes, France. Vinyl ester (VE) plasticizer, lithium cobaltate ( $\text{LiCoO}_2$ ), dimethyl carbonate (DMC), and N-methyl-2-pyrrolidone (NMP) were obtained from Shan-shan Co., Ltd., Changsha, China. Sodium carboxymethyl cellulose (CMC) was manufactured by Tianjing Yuanli Chemical Co., Ltd., Tianjin, China. Styrene-butadiene rubber (SBR) was manufactured by Jilin Chemical Industry Co., Ltd., Jilin, China.

For the fabrication of PVdF-HFP island-coated composite (PIC) separator, PVdF-HFP and ethylene carbonate (EC) were dry-mixed firstly, followed by kneading at 60 °C for 1 h, resulting in pre-swelling PVdF-HFP particles. After that, polyacrylate (PA) binder (5 wt.%) and deionized water were added in turn under vigorous magnetic stirring at room temperature. The slurry was coated onto both sides of the PE separator by micro-gravure printing and dried at 60 °C for 30 min.

For comparison, PVdF-HFP porous-coated (PPC) separator was synthesized by dipping method. PVdF-HFP powders were weighed and dissolved in DMC to form a homogeneous solution by stirring for 1 h at 65 °C. The functional layer was prepared by dipping the PE separator into solution. The residual solvent was evaporated slowly at room temperature with humidity-controlled atmosphere.

The surface morphology was determined by field emission scanning electron microscopy (SEM, Hitachi S-4800, Tokyo, Japan). The separators were measured using a Gurley densometer (Gurley 4110, Gurley Precision Instruments, Troy, NY, USA). Differential scanning calorimetry (DSC) measurements were carried out on a Mettler-Toledo thermogravimetric analysis/differential scanning calorimetry

from 50 to 200 °C at 10 °C/min. Degree of crystallinity ( $\chi_c$ ) of the separator coatings was determined from the DSC curve using the following equation:

$$\chi_c = \frac{\Delta H_f}{\Delta H_f^*} \times 100\% \quad (1)$$

where  $\Delta H_f$  and  $\Delta H_f^*$  are melting enthalpies of the separator coatings and of perfectly crystalline PVdF-HFP, respectively.  $\Delta H_f^*$  can be assumed to be 104.7 J/g [18].

The ionic conductivities were measured by electrochemical impedance spectroscopy (EIS, CHI760D, Shanghai, China). The samples to be tested were cut into round pieces with a diameter of 45 mm and soaked for an hour in liquid electrolyte (1.1 M LiPF<sub>6</sub> in EC/DMC (1/1 by volume)). The resistance ( $R$ ) of pieces of separator was obtained from the low-frequency intercept on the ReZ axis, which was analyzed in the 1 to 10<sup>5</sup> Hz frequency range at 25 °C. The separator was placed in the copper fixture, which underwent surface grinding before use to remove the oxide layer and was sealed with 245 N forces. Each sample was tested repeatedly by changing the thickness from 1 to 4 layers with a correlation coefficient of linear regression ( $R^2$ ) of >0.99. The ionic conductivities ( $\sigma$ ) were calculated using the equation:

$$\sigma = \frac{L}{\bar{R}A} \times 100\% \quad (2)$$

where  $L$  is the thickness of the separator,  $\bar{R}$  is the average resistance of pieces of separator, and  $A$  is the area of the testing electrode. The water contact angle measurements were carried out using a contact angle measuring system (AL200C, Tomey Instruments, Cambridge, MA, USA). The electrolyte uptake was computed using the following equation:

$$EU\% = \frac{w_1 - w_0}{w_0} \times 100\% \quad (3)$$

where  $w_0$  and  $w_1$  are the weights of separator before and after absorbing the liquid electrolyte completely, respectively [19]. The mechanical properties were all tested using an electronic universal testing machine (MTS systems, Eden Prairie, MN, USA) at a speed of 15 mm/min with a 25 mm width. The adhesion strength between the separator and electrodes was measured using a 180° pull-off test for the final commercial pouch cell. The thickness of the middle part of the pouch cells was measured from left to right after the cycling test.

For industrial applications of this technique, ATL's (Amperex Technology Limited, Hong Kong, China) commercial pouch cell was designed with a LiCoO<sub>2</sub>-graphite system. The geometry of the pouch cell was about 3.6 mm in thickness, 3.4 cm in width and 9.1 cm in length, with a nominal capacity of 1800 mAh. The pouch cells were assembled by sandwiching the separator between a LiCoO<sub>2</sub> cathode and a graphite anode. The cathode was prepared by casting a slurry of the active material LiCoO<sub>2</sub> (90 wt.%), conductive carbon (5.0 wt.%), and PVdF (5.0 wt.%) in NMP on aluminum foil. The anode was fabricated by casting a slurry of commercial graphite (96.5 wt.%), conductive carbon (1.0 wt.%), CMC (0.5 wt.%), and SBR (2.0 wt.%) in water on copper foil. The cathode and anode were dried at 85 °C. The active material mass loading and the electrode density of the anode was 9.0 mg/cm<sup>2</sup> and 1.65 g/cm<sup>3</sup>, respectively, and that of the cathode was 19.2 mg/cm<sup>2</sup> and 4.1 g/cm<sup>3</sup>. Before the injection process, the jelly rolls were baked at 80 °C, until the cell contained ≤200 ppm H<sub>2</sub>O. The assembled pouch cells were cycled on a cell testing system (LAND CT2001A, Wuhan LAND electronics Co., Ltd., Wuhan, China) between 3.0 and 4.3 V under different current rates.

### 3. Results and Discussion

A separate adhesive layer (PVdF) is applied to the separator to bond the electrode and separators [20], industrialization by Samsung SDI, LG Chemical, ATL, etc. The amorphous region of PVdF could be swelled by electrolyte uptake and bonded to electrodes during the lamination step [21].

However, good mechanical strength is needed to maintain a microporous structure. It has been reported that mechanical properties will increase 50%–100% by increasing crystallinity degree [22]. Here, a pre-swelling process is developed to balance the swelling degree and mechanical strength, which is schematically illustrated in Figure 1. The PVdF-HFP particles are pre-swelled with EC, using a kneading method, and used to synthesise PVdF-HFP island-coated composite (PIC) separator by micro-gravure printing. The rhombus-mesh structure of anilox roll is beneficial to retain the dispersed polymer particle structure. Typically, a PIC separator retains the “island-like” morphology of PVdF-HFP particles, which are exposed on the surface (Figure 2c,f). For reference, the sample of PE separator and PVdF-HFP porous-coated (PPC) separator are shown in Figure 2a,d,b,e, respectively. The PE separator shows a typical porous structure with a uniform diameter of approximately 20–50 nm, while the PPC separator has a microporous structure with a pore size around 1–8  $\mu\text{m}$ , synthesized using a dipping process. The PIC separator maintains a consistent structure of PVdF-HFP polymer particle for high crystallinity of the coating, which is confirmed by the DSC data (Table 1 and Figure 3a). The endothermic peak for the PIC separator shifts 42 °C negatively, slightly higher than that of PPC separator. Compared with the raw PVdF-HFP material, the PIC separator shows a close crystallinity of 10.61%, while the PPC separator has a relative crystallinity of 2.32%.

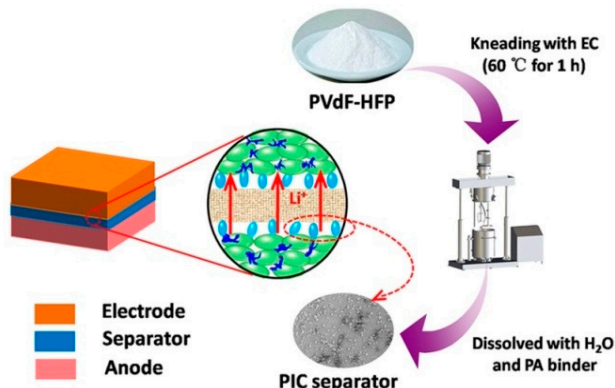


**Figure 1.** Schematic showing the synthesis of the PIC separator.

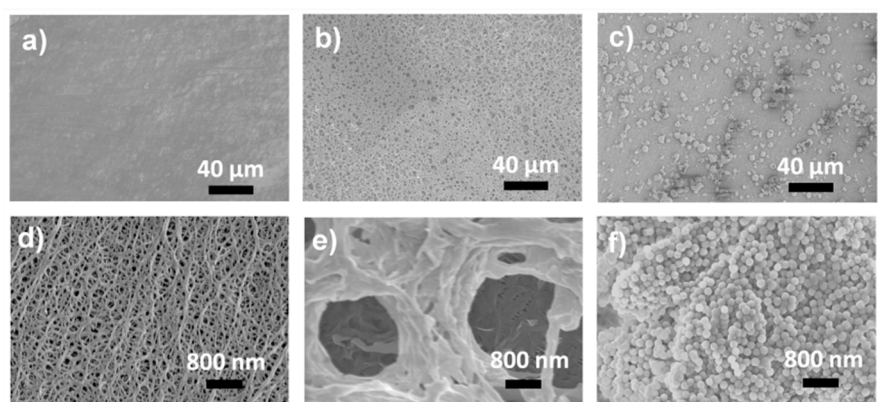


**Figure 2.** Typical SEM images of (a,d) PE separator; (b,e) PPC separator; (c,f) PIC separator.

**Table 1.** DSC data of raw PVdF-HFP materials and separators with different coatings.

| Sample   | $T_m$ (°C) | $\Delta H_f$ (J/g) | $\chi_c$ (%) |
|----------|------------|--------------------|--------------|
| PVdF-HFP | 152.5      | 18.69              | 17.85        |
| PPC      | 99.1       | 2.43               | 2.32         |
| PIC      | 141.1      | 11.11              | 10.61        |

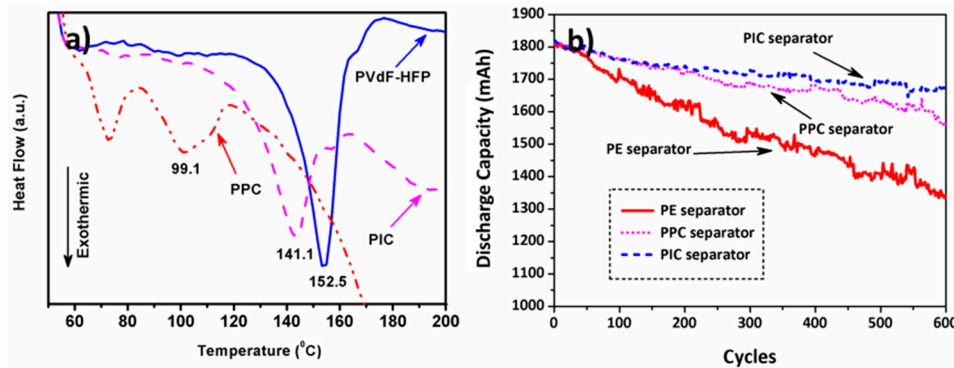


**Figure 3.** Differential scanning calorimetry (DSC) curves (a) and cycle performance (b) of PE separator, PPC separator, and PIC separator.

As reported in previous studies, cosolvents penetrate the semi-crystalline polymer and swell the polymer chains, resulting in the reduction of crystalline phase content with improved affinity of the separator for electrolyte solution and ionic transformation ( $\text{Li}^+$ ) diffusion ability [17,20]. The basic physical and electrical parameters of separators are considered and presented in Table 2. The Gurley value of the PIC separator has the same level as the PE separator, showing high permeability on the “island-like” structure. However, The Gurley value of the PPC modified separator is about twice that of the PE separator. This indicates that some flow paths of the PPC separator may be blocked, which is supported by the high magnification SEM images shown in Figure 2e. The electrolyte uptake and ionic conductivity of separators are crucial for excellent electrochemical performance. Before testing, all samples were fully infiltrated with liquid electrolyte. For the PVdF-HFP coated separators, both the PPC and PIC separator shows superior electrolyte uptake values and ionic conductivities (Table 2 and Figure 4). These are the result of the excellent material properties of PVdF-HFP, such as the porous structure, lyophilic surface, and high dielectric constant [15,23]. It can be seen that the ionic transformation diffusion ability is mainly concerned with the high-affinity surface of coatings for the electrolyte, that is, PPC separator and PIC separator have similar high ionic conductivities, while the amorphous proportions are different.

**Table 2.** Basic physical and electrical parameters of separators.

| Separators | Gurley Value (s/10 mL) | Electrolyte Uptake (%) | Ionic Conductivity (mS/cm) | Contact Angle (°) |
|------------|------------------------|------------------------|----------------------------|-------------------|
| PE         | 7.8                    | 62                     | 0.23                       | 99                |
| PPC        | 14.2                   | 115                    | 0.98                       | 75                |
| PIC        | 8.0                    | 130                    | 0.96                       | 50                |

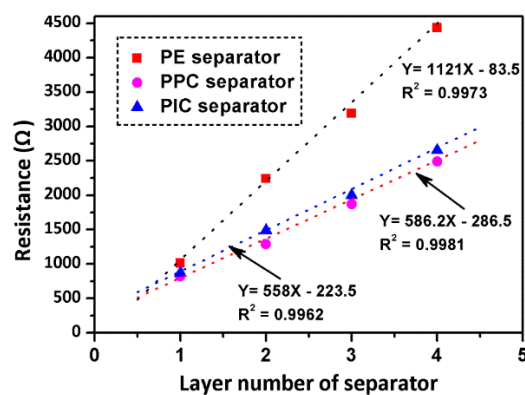


**Figure 4.** The relationship of separator resistance and layer number of separator for PE separator, PPC separator, and PIC separator. The linear fitting results are shown in dotted line.

The cycling performance of pouch cells with PIC separator (Figure 3b) keeps stable at a constant charge/discharge current density ( $0.7\text{C}/1.0\text{C}$  @  $25^\circ\text{C}$ ) up to 600 cycles. For the cell with PIC separator, the capacity retention is 1673 mAh after 600 cycles, whereas the cell with PE separator decreases to 1336 mAh. These results clearly demonstrate that the PIC separator is critical to the long-term reliable performance of the rechargeable battery. We believe that PVdF-HFP coated separators must be present to form a uniform interface, which includes a suitable condition to form a high quality solid electrolyte interphase (SEI) layer and suppress dendrite/mossy lithium growth. As demonstrated in Figure 5, the surface morphology of anode electrodes for cells with PIC separator shows smooth solid particle morphology, whereas a highly rough and loose surface morphology is obtained for conventional cells with PE separator. Furthermore, as mentioned above, the PE separator shows less membrane-electrolyte affinity than the PIC separator. Thus, a smaller meniscus of electrolyte may be formed on the surface of the electrode as described in reference [24].

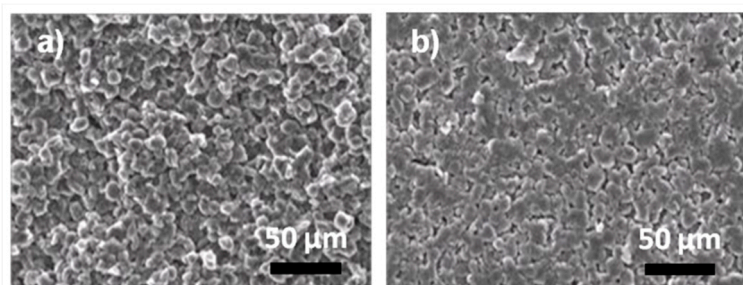


**Figure 5.** SEM images of the top surface morphology of anode electrodes for the pouch cell with (a) PE separator and (b) PIC separator after 10 cycles.

To reveal the mechanism of how PIC separators helped form a homogeneous SEI layer and excellent cycling performance, we tested the pouch cell further. A comparison of the thickness of the middle part of the pouch cell after the 600th cycle is shown in Figure 6. The cells with PIC separator show the typical jelly roll structure of commercial LIB [25], while the cells with PE separator and PPC separator have a periodic wavy-like profile and a pot-shaped profile, respectively. Furthermore, the anode surface of a disassembled cell shows a gray color at the wave site of cells with PE separator, and shows a light-gray color in the middle area of cells with PPC separator (Figure 6 inset). As we all know, the color of anode film is related to Li concentration and phase [26]. The gray color indicates a low concentration of Li in the anode electrode and usually accompanies lithium dendrite at the surface of this area. The interfacial adhesion strength between separator and electrodes is also tested using a  $180^\circ$  pull-off test (Figure 7). It can be seen that the pouch cells with PPC or PIC had the same level of adhesion strength between separator and electrodes, and this was over six times larger than that of the conventional cell. It is also proved that the pre-swelling of the polymer particle surface of the PIC separator could provide enough interfacial adhesion strength between separator and electrodes. For commercial pouch cells, internal stress is engendered during electrochemical process by volumetric expansion of the individual particles in the electrode film. A buckling behavior is displayed resulting in the formation of gaps/voids between electrodes, showing a periodic wavy-like profile [25]. The expanded void/gap in rippled cells needs enough electrolyte to fill it, resulting in the shortage of electrolyte in pouch cells for lithium transportation and the cycling fading [25]. Based on the classical deposition/dissolution model, improving uniformity of lithium distribution and avoiding potential active sites are favourable to inhibiting the growth of lithium dendrite [7]. The separate adhesive layer brings in a stable interfacial structure by intimate contact of the separator to the electrodes [27,28], minimizes the stresses development by strengthening the stiffness, limits interface dislocation between separator and electrode, and finally prevents ripple-shaped deformation.

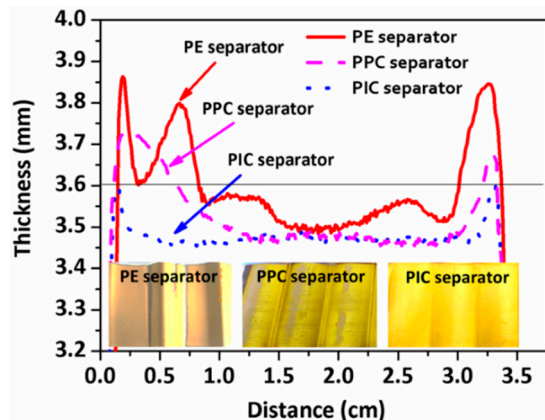


**Figure 6.** The thickness of the middle part of pouch cells with different separators from left to the right after 600th cycle. The inset shows the photographic image of the anode surface of pouch cells after 600th cycling test without any treatment.

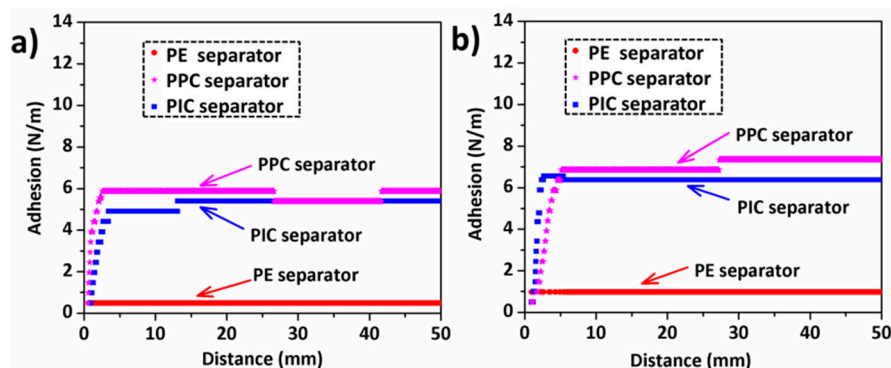


**Figure 7.** The adhesion strength between separator and (a) anode, (b) cathode for pouch cells with different separators.

It should be noted that the pouch cells using PPC separator have low capacity retention (1560 mAh) and a pot-shaped deformation after 600 cycles (Figure 3b). The PPC separator offers a strong face-to-face bonding between electrodes. Then, a tightly-bound structure is formed in the pouch cell, resulting in the internal-stress concentration instead of diffusion. The stress gradient in this pouch cell leads to edge tilting and pot shaping, and can also increase the compaction density of the central part of the electrode [28,29]. This may be the main reason for dendrite growth at the central area of the electrode. In contrast, pre-swelled isolated-polymer island for the PIC separator, not only provides an additional constraining effect for the separator to form a stable and compatible surface between the electrodes, but also eliminates stress concentration by the non-continuous structure (strong point-to-point bonding) to reduce/eliminate pouch cell deformation [30]. Therefore, it may be postulated that the superior interfacial stability with electrodes, along with the well-developed deformation-suppressed structure, allows the PIC separator to prevent dendrite growth and provide a good cycling performance, compared to that of the PPC and PE separator. It should be noted that for the pouch cell with PIC separator, the steady interfacial structure, which is beneficial for lithium diffusion, is considered to be the result of multiple factors. The pre-swelling surface improves the affinity of the separator to the electrolyte solution, and the isolated structure provides enough volume for electrolyte storage. Furthermore, the point-to-point surface structure can balance the high interfacial adhesion of electrodes and anti-deformation ability. To offer optimal electrochemical performance, the size and quantity of the island structure of the PIC separator should be carefully structured and well designed and needs further exploration.

#### 4. Conclusions

In conclusion, we have demonstrated that lithium dendrite growth can be effectively suppressed via a new kind of PVdF-HFP island-coated composite (PIC) separator through a pre-swelling process. The advanced separator not only improved electrolyte wettability and uptake, but also enhanced the interfacial stability of electrodes and anti-deformation ability of pouch cells, which could significantly suppress the growth of lithium dendrites. The pre-swelled polymer surface was beneficial for the interfacial compatibility between PIC separator and electrode materials. The strong point-to-point bonding interfacial adhesion between separator and electrodes significantly smoothed the solid particle morphology of the electrode and prevented ripple-shaped deformation to obtain steady interfacial structure for lithium diffusion. In addition, this non-continuous structure also effectively eliminated stress concentration of the cell and prevented pot-shaped deformation. This paper illustrates a new strategy for the suppression of lithium dendrite growth and opens up a new method for the development of low cost, simple process and easy industry of the lithium-ion pouch cell with improved quality and efficiency.

**Author Contributions:** Conceptualization, J.Z.; Methodology, J.Z., Q.H. and J.W.; Validation, J.Z., P.Z., Y.Z. (Youliang Zhu), Y.Z. (Yongjin Zhao) and M.Y.; Investigation, J.Z., Q.H., Y.Z. (Yongjin Zhao), and M.Y.; Resources, J.Z., Q.H., G.W., Y.L., and L.L.; Data Curation, J.Z., Q.H., Y.Z. (Yongjin Zhao) and M.Y.; Writing-Original Draft Preparation, J.Z., Q.H., J.W., and P.Z.; Supervision, J.Z., G.W., Y.L. and L.L.; Funding Acquisition, J.Z., Y.L. and L.L.

**Funding:** This research was funded by the Scientific Research Fund of Zhejiang Provincial Education Department (No. Y201533679), National Natural Science Foundation of China (Nos. 21476128, 21476127, U1607119), the Public Technology Research Program of Zhejiang Province (GF18B060002), the Scientific and technological Fund from Quzhou Science and Technology Bureau (Nos. 2015Y003, 2016D003, 2017G05, 2017T04), the Personnel Training Foundation of Quzhou University (No. BSYJ201412), the young and middle-aged academic backbone training project (special funds of the construction of teachers' team of Quzhou University) (No. XNZQN201507), and the college students' national innovation and entrepreneurship projects (Nos. 201711488009, 201811488016).

**Conflicts of Interest:** The authors declare no conflicts of interest.

#### References

1. Xu, Q.; Kong, Q.; Liu, Z.; Zhang, J.; Wang, X.; Liu, R.; Yue, L.; Cui, G. Polydopamine-coated cellulose microfibrillated membrane as high performance lithium-ion battery separator. *RSC Adv.* **2014**, *4*, 7845–7850. [[CrossRef](#)]
2. Rasoulis, M.; Vernardou, D. Electrodeposition of vanadium oxides at room temperature as cathodes in lithium-ion batteries. *Coatings* **2017**, *7*, 100. [[CrossRef](#)]
3. Choi, N.S.; Han, J.G.; Ha, S.Y.; Park, I.; Back, C.K. Recent advances in the electrolytes for interfacial stability of high-voltage cathodes in lithium-ion batteries. *RSC Adv.* **2015**, *5*, 2732–2748. [[CrossRef](#)]
4. Zier, M.; Scheiba, F.; Oswald, S.; Thomas, J.; Goers, D.; Scherer, T.; Klose, M.; Ehrenberg, H.; Eckert, J. Lithium dendrite and solid electrolyte interphase investigation using OsO<sub>4</sub>. *J. Power Sources* **2014**, *266*, 198–207. [[CrossRef](#)]
5. Kim, G.T.; Passerini, S.; Carewska, M.; Appetecchi, G. Ionic liquid-based electrolyte membranes for medium-high temperature lithium polymer batteries. *Membranes* **2018**, *8*, 41. [[CrossRef](#)] [[PubMed](#)]
6. Lin, D.; Zhuo, D.; Liu, Y.; Cui, Y. All-integrated bifunctional separator for Li dendrite detection via novel solution synthesis of a thermostable polyimide separator. *J. Am. Chem. Soc.* **2016**, *138*, 11044–11050. [[CrossRef](#)] [[PubMed](#)]
7. Xu, X.; Wang, S.; Wang, H.; Hu, C.; Jin, Y.; Liu, J.; Yan, H. Recent progresses in the suppression method based on the growth mechanism of lithium dendrite. *J. Energy Chem.* **2018**, *27*, 513–527. [[CrossRef](#)]
8. Zhang, Y.; Qian, J.; Xu, W.; Russell, S.M.; Chen, X.; Nasybulin, E.; Bhattacharya, P.; Engelhard, M.; Mei, D.; Cao, R.; et al. Dendrite-free lithium deposition with self-aligned nanorod structure. *Nano Lett.* **2014**, *14*, 6889–6896. [[CrossRef](#)] [[PubMed](#)]
9. Lee, H.; Alcoutlabi, M.; Toprakci, O.; Xu, G.; Watson, J.V.; Zhang, X. Preparation and characterization of electrospun nanofiber-coated membrane separators for lithium-ion batteries. *J. Solid State Electrochem.* **2014**, *18*, 2451–2458. [[CrossRef](#)]
10. Zhang, S.S.; Xu, K.; Jow, T.R. An inorganic composite membrane as the separator of Li-ion batteries. *J. Power Sources* **2005**, *140*, 361–364. [[CrossRef](#)]

11. David, L.; Shareef, K.M.; Abass, M.A.; Singh, G. Three-dimensional polymer-derived ceramic/graphene paper as a Li-ion battery and supercapacitor electrode. *RSC Adv.* **2016**, *6*, 53894–53902. [[CrossRef](#)]
12. Tu, Z.; Kambe, Y.; Lu, Y.; Archer, L.A. Nanoporous polymer-ceramic composite electrolytes for lithium metal batteries. *Adv. Energy Mater.* **2014**, *4*, 1300654. [[CrossRef](#)]
13. Wu, H.; Zhuo, D.; Kong, D.; Cui, Y. Improving battery safety by early detection of internal shorting with a bifunctional separator. *Nat. Commun.* **2014**, *5*, 5193. [[CrossRef](#)] [[PubMed](#)]
14. Li, N.; Wei, W.; Xie, K.; Tan, J.; Zhang, L.; Luo, X.; Yuan, K.; Song, Q.; Li, H.; Shen, C.; et al. Suppressing dendritic lithium formation using porous media in lithium metal-based batteries. *Nano Lett.* **2018**, *18*, 2067–2073. [[CrossRef](#)] [[PubMed](#)]
15. Dong, Z.; Zhang, Q.; Yu, C.; Peng, J.; Ma, J.; Ju, X.; Zhai, M. Effect of ionic liquid on the properties of poly(vinylidene fluoride)-based gel polymer electrolytes. *Ionics* **2013**, *19*, 1587–1593. [[CrossRef](#)]
16. Sousa, R.E.; Kundu, M.; Gören, A.; Silva, M.M.; Liu, L.; Costa, C.M.; Lanceros-Mendez, S. Poly(vinylidene fluoride-co-chlorotrifluoroethylene) (PVDF-CTFE) lithium-ion battery separator membranes prepared by phase inversion. *RSC Adv.* **2015**, *5*, 90428–90436. [[CrossRef](#)]
17. Wu, F.; Feng, T.; Bai, Y.; Wu, C.; Ye, L.; Feng, Z. Preparation and characterization of solid polymer electrolytes based on PHEMO and PVDF-HFP. *Solid State Ion.* **2009**, *180*, 677–680. [[CrossRef](#)]
18. Bandara, T.M.W.J.; Weerasinghe, A.M.J.S.; Dissanayake, M.A.K.L.; Senadeera, G.K.R.; Furlani, M.; Albinsson, I.; Mellander, B.E. Characterization of poly (vinylidene fluoride-co-hexafluoropropylene) (PVdF-HFP) nanofiber membrane based quasi solid electrolytes and their application in a dye sensitized solar cell. *Electrochim. Acta* **2018**, *266*, 276–283. [[CrossRef](#)]
19. Wang, S.; Ajji, A.; Guo, S.; Xiong, C. Preparation of microporous polypropylene/titanium dioxide composite membranes with enhanced electrolyte uptake capability via melt extruding and stretching. *Polymers* **2017**, *9*, 110. [[CrossRef](#)]
20. Santhanagopalan, S.; Zhang, Z.M. Separators for lithium-ion batteries. In *Lithium-Ion Batteries: Advanced Materials and Technologies*; Yuan, X., Liu, H., Zhang, J., Eds.; CRC Press: Boca Raton, FL, USA, 2011.
21. Romanyuk, K.; Costa, C.M.; Luchkin, S.Y.; Kholkin, A.L.; Lanceros-Méndez, S. Giant electric-field-induced strain in PVDF-based battery separator membranes probed by electrochemical strain microscopy. *Langmuir* **2016**, *32*, 5267–5276. [[CrossRef](#)] [[PubMed](#)]
22. Gao, K.; Hu, X.; Dai, C.; Yi, T. Crystal structures of electrospun PVdF membranes and its separator application for rechargeable lithium metal cells. *Mater. Sci. Eng. B* **2006**, *131*, 100–105. [[CrossRef](#)]
23. Seidel, S.M.; Jeschke, S.; Vettikuzha, P.; Wiemhofer, H.D. PVDF-HFP/ether-modified polysiloxane membranes obtained via airbrush spraying as active separators for application in lithium ion batteries. *Chem. Commun.* **2015**, *51*, 12048–12051. [[CrossRef](#)] [[PubMed](#)]
24. Romanyuk, K.; Costa, C.M.; Luchkin, S.Y.; Kholkin, A.L.; Lanceros-Méndez, S. Giant electric-field-induced strain in PVDF-based battery separator membranes probed by electrochemical strain microscopy. *Langmuir* **2016**, *32*, 5267–5276. [[CrossRef](#)] [[PubMed](#)]
25. Zhang, N.; Tang, H. Dissecting anode swelling in commercial lithium-ion batteries. *J. Power Sources* **2012**, *218*, 52–55. [[CrossRef](#)]
26. Shi, B.; Kang, Y.; Xie, H.; Song, H.; Zhang, Q. In situ measurement and experimental analysis of lithium mass transport in graphite electrodes. *Electrochim. Acta* **2018**, *284*, 142–148. [[CrossRef](#)]
27. Liu, Z.; Zhou, J.; Chen, B.; Zhu, J. Interaction between dislocation mechanics on diffusion induced stress and electrochemical reaction in a spherical lithium ion battery electrode. *RSC Adv.* **2015**, *5*, 74835–74843. [[CrossRef](#)]
28. Cannarella, J.; Arnold, C.B. Stress evolution and capacity fade in constrained lithium-ion pouch cells. *J. Power Sources* **2014**, *245*, 745–751. [[CrossRef](#)]
29. Chen, P.H.; Chung, D.D.L. Thermal and electrical conduction in the compaction direction of exfoliated graphite and their relation to the structure. *Carbon* **2014**, *77*, 538–550. [[CrossRef](#)]
30. Darling, K.A.; Tschopp, M.A.; Roberts, A.J.; Ligda, J.P.; Kecskes, L.J. Enhancing grain refinement in polycrystalline materials using surface mechanical attrition treatment at cryogenic temperatures. *Scr. Mater.* **2013**, *69*, 461–464. [[CrossRef](#)]

